# Auger widths of core levels in lithium and sodium

Shyamalendu M. Bose
*Institut de Physique, Université de Liège, Sart-Tilman, B-4000 Liège, Belgium*
*and Department of Physics and Atmospheric Science,* Philadelphia, Pennsylvania 19104*
(Received 20 March 1978; revised manuscript received 30 May 1978)

The Auger widths of the 1*s* core level in lithium and 2*p* core level in sodium are calculated in the renormalized many-body perturbation theory. Calculations have been carried out by using several static and dynamic screenings in the effective Coulomb interaction. Results are found to be very sensitively dependent on the choice of the screening functions.

Recent theoretical and experimental studies of the core-level spectroscopies[1] of metals have emphasized the importance of the finite width of the core levels. In order to explain the experimental data of the soft-x-ray emission and absorption spectra, x-ray photoemission spectra, and the other core-level spectra, theories have predicted a wide range of values for the width of the core states. For example, in Li the quoted values for the width of the core state range from 0.01 through 0.5 eV.

To examine the validity of the various claims one must calculate the widths of the core states by taking into account the different mechanisms that might contribute to such widths. The core broadening can be attributed to several processes. The principal ones are the nonradiative Auger process and the phonon effect.

In this paper we concentrate our attention to the calculation of the Auger widths of the core levels. There have been several previous calculations of the Auger widths in the lowest order of effective Coulomb interaction.[2-4] The level widths for the 1*s* core state in Li and 2*p* core state in Na predicted by these lowest-order theories are too low to explain the experimental results of the deep-level spectroscopies of these metals. Recently Glick and Hagen[5] (GH) went beyond the lowest-order theory for the Auger width and showed that certain higher-order terms were, in fact, divergent. They proposed a renormalized theory for the core-state self-energy. By using a statically screened Coulomb interaction in their numerical evaluation, they showed that the widths of the core states were of the order of 20 meV in both Li and Na.

In this paper we reexamine the renormalized core-state propagator in the presence of several dynamically and statically screened Coulomb interactions and report that the results for the widths of the core states of Li and Na are very sensitively dependent on the choice of the screening functions.

The lowest-order contribution to the core-state self-energy can be expressed in terms of the Feynman diagrams of Fig. 1. In these diagrams downward-directed double lines represent the core-hole propagators. The single lines pointing upward and downward are the propagators for electrons above the Fermi level and those for holes in the conduction band, respectively. Coulomb interactions are represented by the dashed lines. Figure 1(a) corresponds to the production of a particle-hole pair due to polarization of the conduction band by the core hole. Figures 1(b) and 1(c) are the nonradiative Auger process contributing to the core-state self-energy and the corresponding exchange diagram, respectively. These diagrams have been calculated by several authors,[3-5] the most recent calculation being the one by GH. They showed that Fig. 1(a) introduced a fairly large shift (~1 eV) in the core binding energy but did not give rise to a lifetime. In calculating the width of the state from diagrams 1(b) and 1(c), GH found that the results were sensitively dependent on the choice of the wave functions for the conduction electrons. They considered three cases for these wave functions: (a) plane waves, (b) plane waves orthogonalized to the core states and (c) plane waves orthogonalized to a relaxed set of core states, i.e., the core states constructed with one core electron missing. Ob-

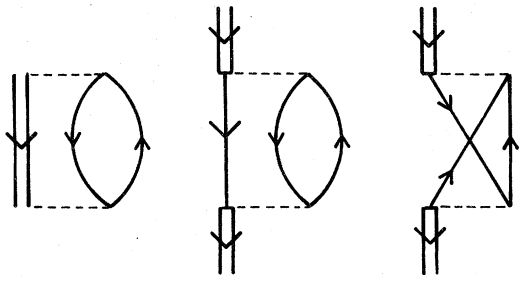

FIG. 1. Lowest-order diagrams for the self-energy of the core state.

 

viously, the last one was the most realistic choice and for this case they obtained the halfwidths of the core states as $0.67\times10^{-4}$ eV for Na and $0.90\times10^{-3}$ eV for Li.

In order to obtain finite results GH used a screened Coulomb potential for the interaction lines. The above results were obtained by using the statically screened Fermi-Thomas interaction. It is, however, well known that Fermi-Thomas screening is too strong at metallic densities and Bohm-Pines screening or a dynamic screening is perhaps a more realistic choice at these densities. In this paper we evaluate the self-energies by introducing dynamic screening. In such a case the width of the core state is obtained from the diagram shown in Fig. 2. This diagram represents the nonradiative Auger process which contributes to the self-energy of the core state. The line of bubbles represents the dynamically screened Coulomb interaction corresponding to excitations of one or more particle-hole pairs in the medium. In particular, we consider the random-phase approximation (RPA) screening of the Coulomb interaction. The imaginary part of the core-state self-energy for Fig. 2 can be written

$$\mathrm{Im}\,\Sigma_B(\omega)=\frac{1}{(2\pi)^6}\int d\vec{k}_v\int d\vec{k}\,\Theta(E_F-E_k)\Theta(E_k-\omega)\times\mathrm{Im}V(\vec{k}_v,\omega-E_k)\times\sum_e|f_e(\vec{k}+\vec{k}_v)|^2, \quad (1)$$

where $f_e(\vec{k}+\vec{k}_v)$ is the vertex function corresponding to the transition from a conduction state of momentum $\vec{k}$ to the core state via a Coulomb interaction of momentum $\vec{k}_v$. The summation over subscript $e$ is introduced to take into account the degeneracy of the core state. This function takes different forms for different choices for the conduction-electron wave functions. This has been discussed in detail by GH. $\mathrm{Im}\,V(k,\omega)$ in Eq. (1) represents the imaginary part of the dynamically screened Coulomb interaction and can be written

FIG. 2. Auger self-energy of the core state in the presence of dynamic screening.

$$\mathrm{Im}\,V(\vec{k},\omega)=-v(\vec{k})\frac{\epsilon_2(\vec{k},\omega)}{\epsilon_1^2(\vec{k},\omega)+\epsilon_2^2(\vec{k},\omega)}, \quad (2)$$

where $v(\vec{k})$ is the bare Coulomb interaction. In the RPA, $\epsilon_1(\vec{k},\omega)$ and $\epsilon_2(\vec{k},\omega)$ are the real and imaginary parts of the dielectric function, respectively.

The angular integrations in Eq. (1) can be carried out analytically and the result can be expressed in terms of dimensionless quantities as

$$\frac{\mathrm{Im}\Sigma_B(\omega)}{4E_F}=12\pi y_p^2\int_0^\infty dv\int_W^{1/2}a\,da\,\mathrm{Im}\left[\frac{1}{\epsilon\left(v,\frac{W^2-a^2}{v}\right)}\right]\times F(a,v), \quad (3)$$

where $y_p=\omega_p/4E_F$, $v=k_v/2k_F$, $a=k/2k_F$, and $W^2=\omega/4E_F$. $F(a,v)$ is the term corresponding to the vertex function $\sum_e|f_e(\vec{k}+\vec{k}_v)|^2$ expressed in a dimensionless form.

In principle, there will be two contributions to $\mathrm{Im}\,\Sigma_B(\omega)$ from Eq. (3): one due to single-particle excitations and the other due to excitation of a plasmon in the medium. For the plasmon excitation, $\mathrm{Im}\,V(k,\omega)$ becomes a representation of the $\delta$-function and plasmon part of the self-energy can be expressed as

$$\left(\frac{\mathrm{Im}\Sigma_B(\omega)}{4E_F}\right)_{\mathrm{pl}}=6y_p^2\int_0^{v_c}\frac{v\,dv}{(\partial\epsilon_1/\partial u)_{u=u_k}}F((W^2-u_kv)^{1/2},v)\times\Theta(0.25-W^2+u_kv), \quad (4)$$

where $u_k=\omega_k/4E_F$ with plasmon frequency $\omega_k$ defined in Ref. 2.

$$\left(\frac{\partial\epsilon_1}{\partial u}\right)_{u=u_k}=\frac{3y_p^2}{4v3}\left((u_k-v)\ln\left|\frac{u_k-v-1}{u_k-v+1}\right|+(u_k+v)\ln\left|\frac{u_k+v+1}{u_k+v-1}\right|\right). \quad (5)$$

It should be pointed out that on the energy shell, i.e., for $\omega=\omega_B$, the plasmon [Eq. (4)] would not contribute to $\mathrm{Im}\,\Sigma_B(\omega_B)$. The single-particle contribution to $\mathrm{Im}\,\Sigma_B(\omega_B)$ is obtained from Eq. (3). Final two-dimensional integrals in Eq. (3) and the single integral over $v$ in Eq. (4) for the plasmon contribution have been carried out numerically. Calculations have been done with the vertex function $F(a,v)$ evaluated for three different wave functions for the conduction electrons: (i) plane waves, (ii) plane waves orthogonalized to the core states; (iii) plane waves orthogonalized to the relaxed core-hole states. The results for the halfwidth of the core states, i.e., $\mathrm{Im}\,\Sigma_B(\omega_B)$ for Na and Li are shown in Table I. These results are on the same order of magnitude as the results of GH for the corresponding cases. The difference must be attributed to the difference in the choice of the screenings of the effective potentials used in these calculations. In any case, both calcula-

TABLE I. Auger widths of the $2p$ core level of sodium and $1s$ core level of lithium for various choices of conduction-electron wave functions.

| Wave function orthogonalized | Relaxed | $\Gamma_0$ (eV) = Im $\Sigma_B(\omega_B)$ Na | Li |
|---|---|---|---|
| no | no | $2.28\times10^{-3}$ | $3.94\times10^{-3}$ |
| yes | no | $1.0\times10^{-4}$ | $2.12\times10^{-3}$ |
| yes | yes | $1.25\times10^{-4}$ | $1.25\times10^{-3}$ |

tions yield results which are too small to explain the experimental x-ray spectra of Na and Li.

Glick and Hagen then examined the higher-order processes which could contribute to the Auger width of the core states. They found that the diagram shown in Fig. 3 introduced a divergent contribution to the core-hole width. Realizing that this diagram could be viewed as a correction to Fig. 1(a), they proceeded to renormalize the internal core-hole line of Fig. 1(a), i.e., they calculated the core-hole self-energy from Fig. 4(a). The cross-hatched double line in this figure represented the renormalized core-hole propagator satisfying the Dyson equation of Fig. 4(b). The self-energy part in this figure was obtained from the diagrams of Fig. 1. Glick and Hagen again used a statically screened Coulomb interaction corresponding to Fermi-Thomas screening for the interaction lines and obtained a self-consistent solution of Fig. 4(a). For both Na and Li they found that the half widths of the core holes were on the order of 20 meV. For Li this result was one order of magnitude larger than the previously calculated values and for Na it was several orders larger than the best previous Auger value.

It is somewhat surprising that a renormalization procedure of the internal core-hole propagator of the self-energy diagram should bring about such a huge change in the width of the core states. Thus, in order to establish the validity of the

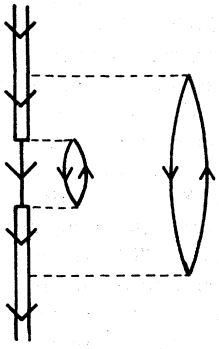

FIG. 3. Higher-order diagram which introduces a divergent contribution to self-energy of the core state.

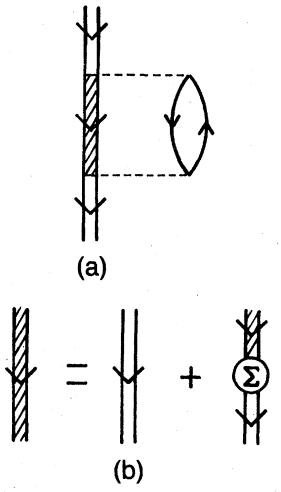


FIG. 4. (a) Diagram for the self-energy of the core state with a renormalized core-hole propagator. (b) Schematic representation of the Dyson's equation satisfied by the renormalized core-state propagator.

results of GH, we decided to evaluate the core-state widths in the renormalized theory by introducing several modifications in the effective Coulomb interactions. First, we note that Fermi-Thomas screening is known to be too strong at metallic densities and is supposed to be reasonable only for describing long-range phenomena, i.e., phenomena involving small momentum transfers. However, since the core state is localized in space, all wave numbers up to the inverse of the core radius should contribute to the calculation of core-state self-energy. Thus, as a first step towards incorporating, at least partially, the short-range and local field effects we now study the self-energy of the core state in the presence of the effective Coulomb interaction screened by the RPA screening function. The RPA introduces the most simple form dynamic screening and the appropriate diagram for the calculation of the self-energy in this approximation is shown in Fig. 5. The line of bubbles, in this diagram, represents the RPA Coulomb interaction and the cross-hatched double line again represents the renormalized core-hole propagator.

The contribution of Fig. 5 to the imaginary part

FIG. 5. Diagram for the renormalized theory of the core-state self-energy in the presence of dynamic screening.

of the self-energy can be written

$$\mathrm{Im}\,\Sigma_B^R(\omega)=\frac{2}{(2\pi)^4}\int_\omega^\infty d\omega'\int d\vec{k}_v\sum_{i,e}|g_{ie}(\vec{k}_v)|^2\,\mathrm{Im}\,V(\vec{k}_v\omega-\omega')\,\frac{\mathrm{Im}\Sigma_B(\omega')}{[\omega'-E_B-\mathrm{Re}\Sigma_B(\omega')]^2+\mathrm{Im}\Sigma_B^2(\omega')}. \tag{6}$$

The matrix element $g_{ie}(\vec{k}_v)$ represents the vertex function where two core-hole lines meet a Coulomb line. Summation over indices $i$ and $e$ is introduced to incorporate degeneracy of the core state. The function $g_{ie}(\vec{k}_v)$ has been studied before.[2,5] The halfwidth of the core state is obtained by evaluating Eq. (6) on the energy shell, i.e., by replacing $\omega$ by $\omega_B$ in Eq. (6). In such a case this expression takes the approximate form

$$\mathrm{Im}\Sigma_B^R(\omega_B,\mathrm{Im}\,\Sigma_B)=\int_{-\infty}^0 d\omega\int d\vec{k}_v\,\mathrm{Im}\,V(\vec{k}_v,\omega)\times\frac{\mathrm{Im}\,\Sigma_B(\omega_B)}{\omega^2+\mathrm{Im}\,\Sigma_B^2(\omega_B)}\times\sum_{i,e}|g_{ie}(\vec{k}_v)|^2. \tag{7}$$

The angular integrations in Eq. (7) can be carried out analytically. $\mathrm{Im}\,\Sigma_B^R(\omega_B,\mathrm{Im}\,\Sigma_B)$ has two contributions corresponding to the single-particle excitation and the plasmon excitation in the medium. These two contributions can be expressed in terms of dimensionless quantities as

$$\left.\frac{\mathrm{Im}\,\Sigma_B^R(\omega_B,\Gamma_B)}{4E_F}\right|_{\mathrm{sp}}=\frac{6y_p^2}{\pi}\int_{-\infty}^0 d\xi\int_{v_{\min}}^{v_{\max}}dv\,\frac{\epsilon_2(v,\xi)}{\epsilon_1^2(v,\xi)+\epsilon_2^2(v,\xi)}\,\frac{\Gamma_B}{\xi^2+\Gamma_B^2}\,G^2 \tag{8}$$

and

$$\left.\frac{\mathrm{Im}\,\Sigma_B^R(\omega_B,\Gamma_B)}{4E_F}\right|_{\mathrm{pl}}=6y_p^2\int_0^{v_c}dv\,\frac{v}{(\partial\epsilon_1/\partial u)_{u=u_k}}\,\frac{\Gamma_B^2}{(vu_k)^2+\Gamma_B^2}\,G^2. \tag{9}$$

Here

$\xi=\omega/4E_F$, $v=k_v/2k_F$, $v_{\min}=-0.5+(0.25-\xi)^{1/2}$, $v_{\max}=0.5+(0.25-\xi)^{1/2}$ and $v_c=k_c/2k_F$

where $k_c$ is cutoff wave number for plasmon production. $G^2$ represents $\sum_{i,e}|g_{ie}(k_v)|^2$ expressed in dimensionless units. Also $\Gamma_B$ in Eqs. (8) and (9) is the core-hole width $\mathrm{Im}\,\Sigma_B(\omega_B)$ expressed in units of $4E_F$.

Obviously the total contribution to the self-energy is obtained from

$$\mathrm{Im}\,\Sigma_B^R(\omega_B,\Gamma_B)=\mathrm{Im}\,\Sigma_B^R(\omega_B,\Gamma_B)|_{\mathrm{sp}}+\mathrm{Im}\,\Sigma_B^R(\omega_B,\Gamma_B)|_{\mathrm{pl}}. \tag{10}$$

To obtain the core-hole width $\Gamma$ one must solve Eq. (10) self-consistently. This would require that we evaluate $\mathrm{Im}\,\Sigma_B^R$ as a function of $\Gamma_B$ from Eqs. (8), (9), and (10) and then apply the self-consistency requirement that $\Gamma$ is obtained from the equation

$$\Gamma=\Gamma_0+\mathrm{Im}\,\Sigma_B^R(\omega_B,\Gamma), \tag{11}$$

where

$$\Gamma_0=\mathrm{Im}\,\Sigma_B(\omega_B).$$

The results of our numerical calculations for $\mathrm{Im}\,\Sigma_B^R$ for Li and Na are plotted in Figs. 6 and 7. We then solve Eq. (11) graphically to obtain

$\Gamma_{\mathrm{RPA}}=0.54$ eV for Li,

$\Gamma_{\mathrm{RPA}}=0.86$ eV for Na.

Thus the renormalized theory in the presence of the RPA screened Coulomb interaction gives level widths which are approximately 25 and 40 times larger than those obtained by GH for Li and Na, respectively.

In several recent papers[1,6,7] it is pointed out that the x-ray emission and absorption data of Li can be explained satisfactorily by assuming

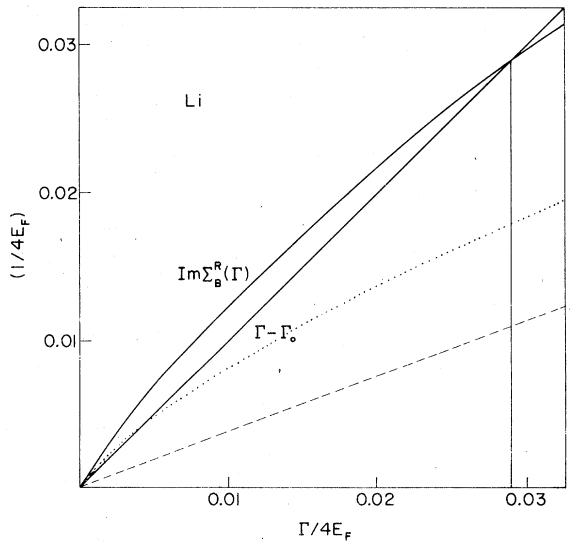


FIG. 6. Imaginary part of the self-energy (solid curve) $\Sigma_B^R$ of the 1s core state in Li due to Fig. 5 plotted against $\Gamma_B$. Intersection of the curve and the straight line gives the 1s core-level width in Li. The single-particle and the plasmon contribution to $\mathrm{Im}\,\Sigma_B^R$ are shown by the dotted and dashed curves, respectively.

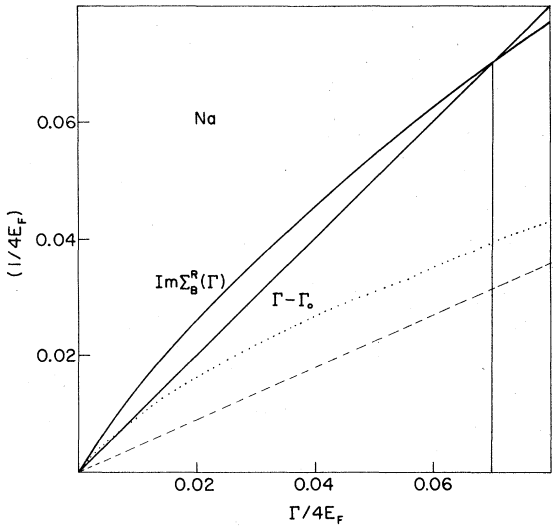


FIG. 7. Imaginary part of the self-energy (solid curve) $\Sigma_B^R$ of the $2p$ corve level in Na due to Fig. 5 plotted against $\Gamma_B$. Intersection of the curve and the straight line gives the $2p$ core-level width in Na. The single-particle and the plasmon contributions to $\mathrm{Im}\Sigma_B^R$ are shown by the dotted and dashed curves, respectively.

a lifetime width of the 1s core state as $0.03 \pm 0.02$ eV. This obviously gives credence to the results of GH. On the other hand several previous calculations[8,9] have indicated that the Li x-ray data can be explained by a 1s core level width of 0.3–0.5 eV. If this were true, our result would not be so unrealistic.

Glick and Hagen have calculated the level width from the single bubble diagram for the self-energy. To obtain finite results they have used a statically screened Coulomb potential for the interaction lines. In this paper we have replaced these Coulomb interaction lines and the single bubble diagram by a dynamically screened Coulomb interaction line. Thus, these two calculations basically include the same processes contributing to the Auger width, although the RPA is somewhat more realistic since it introduces dynamic effects. We excepted that the results in these two calculations would be of the same order of magnitude. The big difference in these two results is surprising. At this point we must point out that, like the Fermi-Thomas potential, the RPA theory is also poor for short-range and local-field effects. Although it retains terms to all orders of perturbation theory, it keeps only those terms which are important for small momentum transfer. However, as pointed out before for calculations involving the core states, large momentum transfer terms must also be retained. For such large momentum transfers, exchange terms and other higher-order graphs can become as important as the RPA graph. In an effort to check whether the exchange terms would, in fact, alter the core-state self-energy significantly, we have recalculated the core-level widths by using the Hubbard[10] exchange correction in the screening function, i.e., we have used the modified dielectric function

$$\epsilon(\vec{k}, \omega) = 1 + Q_0(\vec{k}, \omega)/[1 - G(\vec{k})Q_0(\vec{k}, \omega)] \qquad (12)$$

in our theory. Here $G(\vec{k})$ is the Hubbard exchange correction factor and is given by

$$G(\vec{k}) = \tfrac{1}{2}k^2/(k^2 + k_F^2) \qquad (13)$$

and

$$Q_0(\vec{k}, \omega) = -v(\vec{k})\chi^0(\vec{k}, \omega),$$

where $v(\vec{k})$ is the Coulomb interaction and $\chi^0(\vec{k}, \omega)$ is the usual free-electron polarizability. The final results are again obtained self-consistently by solving Eq. (11) by graphical methods and are found to be

$$\Gamma_H = 1.41 \text{ eV for Li},$$

$$\Gamma_H = 1.47 \text{ eV for Na}.$$

These results are larger than those of the RPA theory. Thus the results for the core-state widths obtained by evaluating Fig. 5 become progressively worse as we use more and more realistic screenings of the Coulomb interaction.

As a last attempt to obtain realistic values of the core-level widths we have used another statically screened Coulomb interaction. From an elaborate treatment of the many-body perturbation theory, Bohm and Pines[11] showed that the effective electron interaction in a metal could be roughly represented by a Yukawa-type potential where the screening constant is given by

$$k_c^2 = 4\pi m e^2/\hbar\omega_p .$$

Using such a screened Coulomb interaction in the GH theory we have reevaluated the level widths and have found the following results

$$\Gamma_{BP} = 0.912 \text{ eV for Li},$$

$$\Gamma_{BP} = 1.029 \text{ eV for Na}.$$

These values are also unacceptably large and are clearly inconsistent with the observed soft x-ray spectra of lithium and sodium.

In conclusion, we observe that the Auger widths calculated by using the renormalized propagator of Fig. 5 are extremely sensitive to the choice of the effective electron interactions. Of the various values evaluated, those obtained by using the Fermi-Thomas screening factor appear to be consistent with the observed soft x-ray spectra of

lithium and sodium. However, for reasons discussed above, Fermi-Thomas screening is perhaps the poorest of all the screening functions discussed in this paper. Thus the result obtained by using this screening function cannot be accepted as the true value of the Auger level widths. The other screening functions are known to be more realistic even though each one of them gives unacceptable values for the level widths as obtained from Fig. 5. This situation leads us to believe that there are other higher-order diagrams which are as important as those considered by GH and the present author. Some of the higher-order terms must introduce significant cancellation in the core-state level widths. The importance of cancellation terms on the soft x-ray spectra of metals has been emphasized by various authors.[12-14] We conclude with the conjecture that the true value of the Auger widths of the core states can only be obtained by considering the graph of Fig. 5 along with the appropriate higher-order terms.

ACKNOWLEDGMENT

This work was performed under the auspices of the International Center for Theoretical Solid State Physics (University of Antwerp–UIA and University of Liège) in the framework of the joint project ESIS (Electronic Structure in Solids).

---

*Present address.

[1]P. H. Citrin, G.K. Wertheim, and Y. Baer, Phys. Rev. B 16, 4256 (1977), and references therein.
[2]S. M. Bose, Ph.D. thesis (University of Maryland, 1967); S. M. Bose and A. J. Glick, Phys. Rev. B 10, 2733 (1974).
[3]B. Bergersen, P. Jena, and T. McMullen, J. Phys. F 4, L219 (1974).
[4]T. Kobayasi and A. Morita, J. Phys. Soc. Jpn. 28, 457 (1970).
[5]A. J. Glick and A. L. Hagen, Phys. Rev. B 15, 1950 (1977).
[6]T. A. Callcott and E. T. Arakawa, Phys. Rev. Lett. 38, 442 (1977).
[7]C.-O. Almbladh, Phys. Rev. B 16, 4343 (1977).
[8]A. J. McAlister, Phys. Rev. 186, 595 (1969).
[9]G. D. Mahan, Phys. Rev. B 11, 4814 (1975).
[10]J. Hubbard, Proc. R. Soc. London, Ser. A 243, 336 (1957).
[11]D. Bohm and D. Pines, Phys. Rev. 92, 609 (1953).
[12]P. Longe and A. J. Glick, Phys. Rev. 177, 526 (1969).
[13]B. Bergersen, F. Brouers, and P. Longe, J. Phys. F 1, 945 (1971).
[14]S. M. Bose and P. Longe, Phys. Rev. B 18, 3921 (1978).